8-22-2019

Paleoclimate of the subtropical Andes during the latest Miocene, Lauca T Basin, Chile

Melina Feitl
University of Nebraska- Lincoln, mfeitl@huskers.unl.edu

Andrea K. Kern
University of São Paulo, São Paulo

Amanda Jones
University of Nebraska - Lincoln, acjones9393@hotmail.com

Sherilyn C. Fritz
University of Nebraska - Lincoln, sfritz2@unl.edu

P. A. Baker
Duke University, pbaker@duke.edu

See next page for additional authors

Palaeogeography, Palaeoclimatology, Palaeoecology 534 (2019) 109336

Contents lists available at ScienceDirect

Palaeogeography, Palaeoclimatology, Palaeoecology

journal homepage: www.elsevier.com/locate/palaeo

Paleoclimate of the subtropical Andes during the latest Miocene, Lauca Basin, Chile

Melina Feitl[a,*], Andrea K. Kern[b], Amanda Jones[a], Sherilyn C. Fritz[c], Paul A. Baker[d], R.M. Joeckel[e,g], Wout Salenbien[d], Debra Willard[f]

[a] Department of Earth and Atmospheric Sciences, University of Nebraska-Lincoln, Lincoln, NE 68588-0340, USA
[b] Department of Sedimentary and Environmental Geology, University of São Paulo, São Paulo, Brazil
[c] Department of Earth and Atmospheric Sciences, School of Biological Sciences, University of Nebraska-Lincoln, Lincoln, NE 68588-0340, USA
[d] Division of Earth and Ocean Sciences, Duke University, Durham, NC 27708, USA
[e] Conservation and Survey Division, School of Natural Resources, Department of Earth and Atmospheric Sciences, University of Nebraska-Lincoln, Lincoln, NE 68588, USA
[f] Climate Research & Development, USGS, Reston, VA 20192, USA
[g] University of Nebraska State Museum, University of Nebraska-Lincoln, Lincoln, NE 68588, USA

ARTICLE INFO

Keywords:
Paleolimnology
Paleolake
Paleoenvironments
Altiplano

ABSTRACT

Uplift of the Andean Cordillera during the Miocene and Pliocene produced large-scale changes in regional atmospheric circulation that impacted local ecosystems. The Lauca Basin (northern Chilean Altiplano) contains variably fluvial and lacustrine sedimentary sequences spanning the interval from 8.7 to 2.3 Ma. Field samples were collected from paleo-lacustrine sediments in the basin. Sediments were dated using detrital zircon geochronology on volcanic tuffs, yielding an age range between ~5.57 and 5.44 Ma. These new age constraints provided an opportunity to evaluate changes in the Lauca Basin ecosystem across this dynamic Miocene-Pliocene transition. We employed multiple proxies (lithofacies analysis, diatoms, pollen, and oxygen stable isotopes of authigenic carbonates) to interpret ancient lacustrine and terrestrial paleoenvironments. Alternations among mudstone, carbonate, and evaporitic facies indicate lake-level variability through time. The diatom assemblage is characterized by meso- to hypersaline and alkaline-tolerant taxa typical of shallow lakes. The $\delta^{18}O$ values ranged from −8.96 to −2.22‰ indicating fluctuations in water balance. Pollen taxa in the outcrop are typical of a transitional stage between seasonal cloud forest and open grassland. Together, these proxies indicate that the Lauca paleolake sediments were deposited under a wetter-than-modern climate with high temporal variability. Our results refine previous studies in the Lauca Basin and are consistent with other regional studies suggesting that the South American summer monsoon at the Miocene-Pliocene transition was more intense than it is at present.

1. Introduction

Major changes in the Earth's topography, climate, and oceanic circulation took place throughout the course of the Miocene and Pliocene epochs (Quade et al., 1995; Gregory-Wodzicki, 2000; Zachos et al., 2001; Zhisheng et al., 2001; Garzione et al., 2006; Ghosh et al., 2006; Mulch et al., 2010; Zhang et al., 2013; Brierly and Fedorov, 2016). High global CO_2 concentrations, perhaps > 450 ppm at the Miocene-Pliocene boundary, were partly responsible for global surface temperatures ~3 °C higher than today, sea level was ~25 m higher than present, and latitudinal sea surface temperature (SST) gradients were lower-than-modern (Fedorov et al., 2006, 2013). The Pacific Ocean may have had El Niño-like conditions in the early Pliocene, with lower-than-modern longitudinal SST gradients across the equator, consequently altering the global distribution of temperature and precipitation (Wara et al., 2005; Fedorov et al., 2006, 2013; Brierly et al., 2009).

The Andean Cordillera exceeds 4500 masl today over most of the range and forms a major longitudinal orographic barrier (Fig. 1). The Altiplano (ca.14–23° S) likely reached its present elevation by the late Miocene (Garzione et al., 2006; Ghosh et al., 2006; Poulsen et al., 2010; Garzione et al., 2014). Uplift of the Andes brought about intensification of the South American summer monsoon (SASM), increasing precipitation in the lowland subtropics and Andean foothills (Lenters and Cook, 1995; Ehlers and Poulsen, 2009; Garreaud et al., 2009). Yet, in

* Corresponding author.
E-mail addresses: mfeitl@huskers.unl.edu (M. Feitl), sfritz2@unl.edu (S.C. Fritz), pbaker@duke.edu (P.A. Baker), rjoeckel3@unl.edu (R.M. Joeckel), wout.salenbien@duke.edu (W. Salenbien), dwillard@usgs.gov (D. Willard).

https://doi.org/10.1016/j.palaeo.2019.109336
Received 3 March 2019; Received in revised form 31 July 2019; Accepted 15 August 2019
Available online 22 August 2019
0031-0182/ Published by Elsevier B.V.

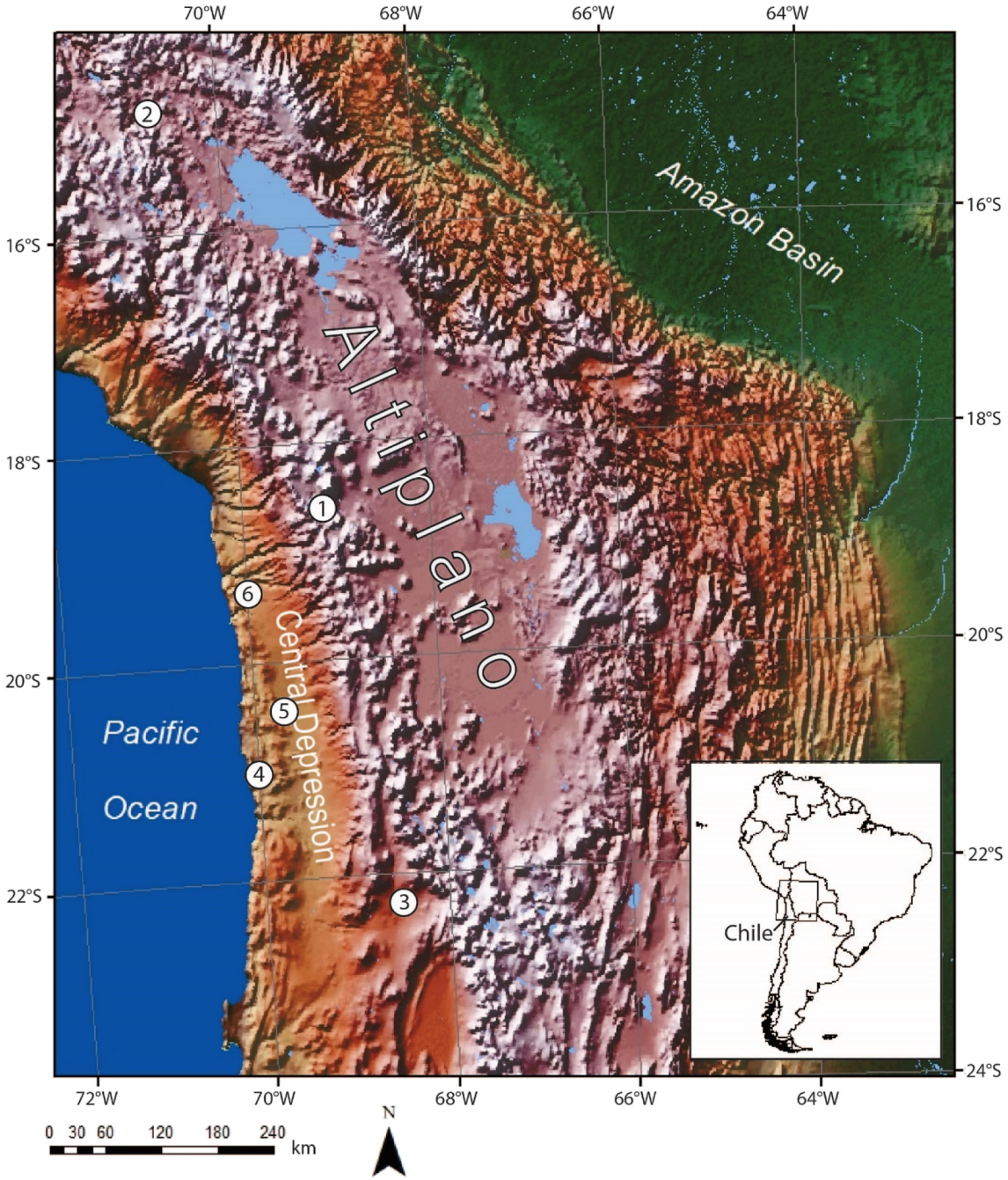

Fig. 1. Relief map (30 arc-second DEM of South America (Data Basin Dataset), U.S. Geological Survey's Center for Earth Resources Observation and Science (EROS)) of the Altiplano and Central Andes in South America, whose extent is indicated by the box on the inset map. Sites described in the text are numbered. (1) Lauca Basin (2) Descanso-Yaurí Basin (3) Calama Basin (4) Salar Grande (5) Quillagua-Llamara Basin (6) Tiliviche Paleolake.

the central Andes, high topography was associated with colder, drier climates (Garreaud et al., 2009).

Miocene-Pliocene lake sediments are not widespread on the Andean Altiplano, limiting opportunities for finer-scale reconstruction of past climate and the effects of tectonic and climate change on past ecosystems. Prior studies from northern Peru to northern Chile suggest a wetter-than-modern late Miocene climate that became more arid approaching the early Pliocene (Kött et al., 1995; Chong et al., 1999; Gaupp et al., 1999; May et al., 1999; Sáez et al., 1999; de Wet et al., 2015; Vélez et al., 2017). In northern Peru, this trend toward aridity was periodically interrupted by wet episodes (Vélez et al., 2017).

The Lauca Basin (Figs. 1, 2) contains one of the highest (averaging 4100 masl) and westernmost Miocene-Pliocene sedimentary successions in the northern Chilean Andes. Sediments of the Lauca Formation span the interval from 8.7 to 2.3 Ma. Within this expansive formation, sediments deposited between 6.4 and 3.7 Ma record the response of an ephemeral lake to changes in the local precipitation-evaporation balance (Gaupp et al., 1999). In this study we examine a portion of the Lauca Formation in higher resolution than in prior studies (Gaupp et al., 1999), integrating sedimentology, petrology, fossil diatoms, palynology, and isotope geochemistry to refine reconstructions of the paleoenvironments and inference of past climates.

2. Study area

The Lauca Basin is the westernmost sub-basin of the Miocene-

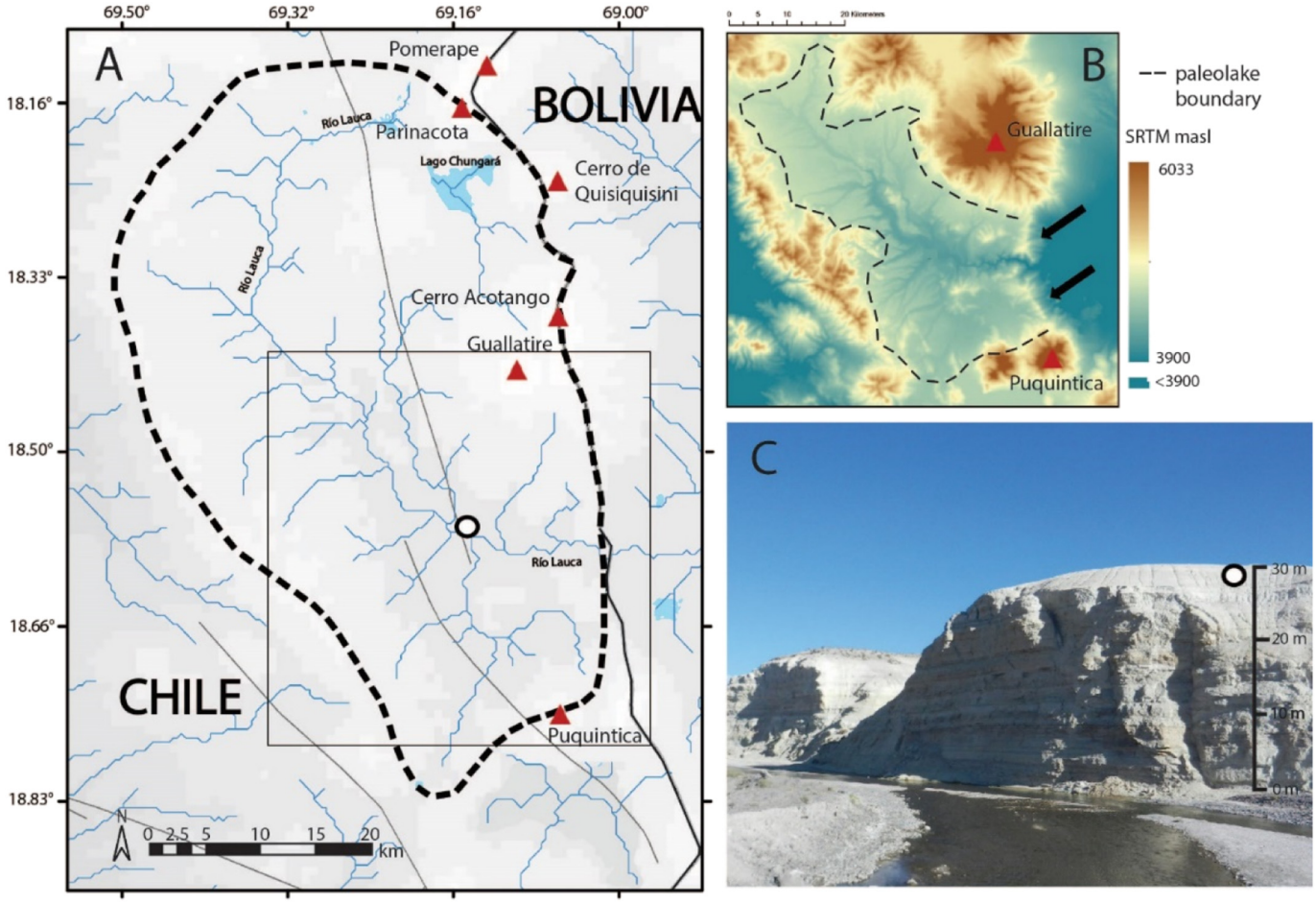

Fig. 2. A) Modern hydrology and outcrop location within the Lauca Basin (1 in Fig. 1). B) Shuttle Radar Topography Mission (SRTM) map of the possible paleolake extent. Black arrows indicate location of the damming of the river by pyroclastic flow. C) Field photograph of outcrop used for representative stratigraphic column (Fig. 5).

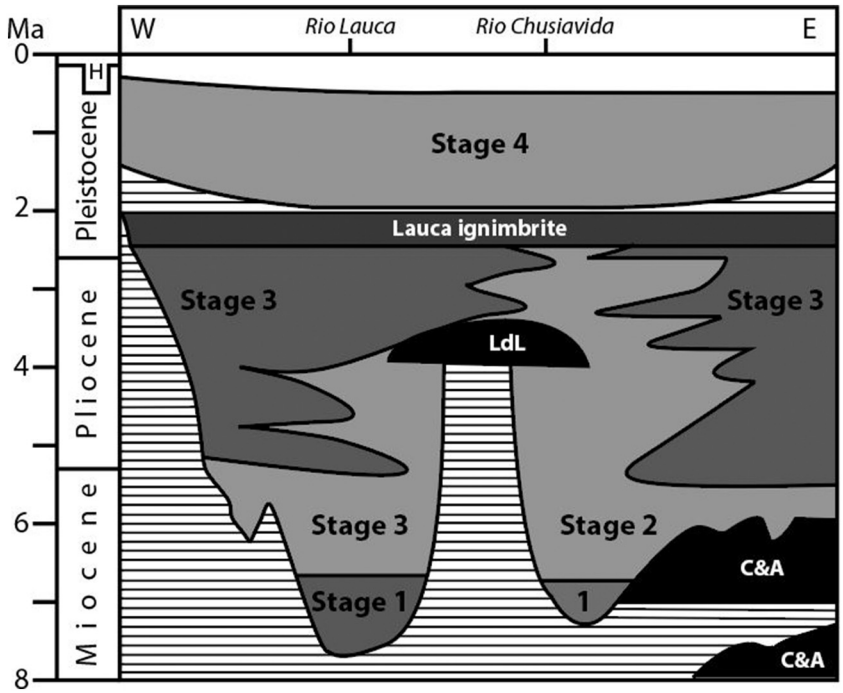

Fig. 3. Regional chronostratigraphy of the Lauca Basin modified after Gaupp et al. (1999). LdL = Lomas de Laucasirca, C. Lliza & El Rojo Norte (3.0–2.3 Ma). C&A = Choquelimpie (6.6 Ma) & Ajoya (7.0 Ma). Periods of non-deposition or erosion indicated by the horizontal lines.

Pliocene fluvio-lacustrine basins on the Altiplano and lies between the active eastern Andean volcanic front and eroded western Miocene volcanoes (Figs. 1, 2) (Gaupp et al., 1999). Volcanic sediments comprising much of the basin fill are dominantly dacitic or rhyolitic ash with volcaniclastic fragments (Wörner et al., 1988; Gaupp et al., 1999). The basin fill, informally known as the Lauca Formation, includes ~120 m of siliciclastic, carbonate, and evaporitic sediments, representing saline lacustrine, alluvial fan, and fluvial sediments deposited under arid to semi-arid conditions (Kött et al., 1995). The relative absence of deformation suggests that vertical changes in facies are likely unrelated to tectonic and volcanic events and instead represent changes in climate (Gaupp et al., 1999). The sedimentary succession of the Lauca Formation unconformably overlies the Quebrada Macusa Formation (~11 Ma), and it is overlain by the Lauca Ignimbrite (2.3 ± 0.7 Ma) (Fig. 3) (Charrier et al., 2005; García et al., 2011).

Today, northern Chile is located in a transition zone with a strong northeast to southwest seasonal precipitation gradient (Arroyo et al., 1988; Garreaud, 2009; Garreaud et al., 2009). The northeastern region, including the Altiplano, is dominated by rainfall in the austral summer (December to March); water vapor in the region originates from the Atlantic Ocean and is influenced by dynamics of the SASM (Garreaud, 2009; Garreaud et al., 2009). In the southwest, precipitation is influenced by the position of the Polar Front and the associated transport of moisture from the southwest during austral winter (May to August). Southwestern air masses are influenced by the Humboldt Current (Peru Current) and cold upwelling, which increases aridity along the northern coast of Chile (Arroyo et al., 1988). In the Lauca Basin today, rainfall occurs primarily during austral summer, with a mean annual precipitation > 300 mm (Rundel and Palma, 2000). Although rainfall shows high seasonality, temperature remains approximately constant during the year, fluctuating from 25 °C during the day to freezing night temperatures, with a mean annual temperature of ~5.1 °C at 4400 masl (Rundel and Palma, 2000).

3. Methods

A single, 31-m thick-sedimentary outcrop (Fig. 2C) from the Lauca Formation (18.5799° S, 69.1606° W, ca. 4065 m above sea level) was sampled in November 2014 along the southwestern bank of the Río Lauca (Fig. 2A). This section corresponds to part of stratigraphic Stage 2 between numbered localities 28 and 36 of Gaupp et al. (1999) (Fig. 3). Thirty-six representative samples of the outcrop lithofacies were collected, and the elevation of each sample was recorded with a hand-held level. Five supplementary samples were collected adjacent to the outcrop.

3.1. Chronology

Ages for samples near the base and top of the outcrop (LB-5 and LB-36) were established through detrital zircon geochronology on volcanic tuffs. Measurements were made at the Arizona LaserChronCenter of the University of Arizona by laser ablation–multicollector–inductively coupled plasma–mass spectrometry (LA-MC-ICP-MS) following established procedures (Gehrels, 2014). This analysis entailed, for both samples, that zircons were extracted from the sediments by crushing and grinding. Zircon grains were subsequently separated from the rest of the matrix by Wilfley table, heavy liquids, and a Frantz magnetic separator. The zircon grains were then mounted in an epoxy puck alongside three primary standards (Sri Lanka, FC-1, R33), prior to being abraded down to a depth of ~20 μm and polished. Pucks were imaged using back-scattered electron images (BSE) and cathode luminescence (CL).

For sample LB-5, a total of 50 unknowns were targeted for LA-ICP-MS analyses, whereas 28 unknown grains were targeted for sample LB-36. For sample LB-5, 46 out of 50 dates were retained for age calculation. Sample LB-36 had 27 out of 28 dates retained for age calculation. Ages were not retained if their ages were discordant (outside of the 95% confidence interval of their age group). Maximum depositional ages were determined by grouping the youngest significant age group and calculating a pooled age from this subset. The true depositional age is likely younger than this maximum age constraint, which should be interpreted as a hard-maximum age. These data are compared to and integrated with earlier ages from the site derived from K/Ar geochronology (Kött et al., 1995; Gaupp et al., 1997; Wörner et al., 2000).

3.2. Sedimentology and petrology

Hand samples were systematically described and integrated with field observations from one section (Fig. 2C) to generate a representative stratigraphic column. Sample descriptions included color in wet and dry conditions (Munsell Color, 2010), reaction with 10% HCl, and descriptions of lithology and sedimentary features.

Twelve of the 41 hand samples were selected for thin-section petrography; collectively, they are considered representative of the range of lithofacies described in this study. These samples are, in ascending stratigraphic order: LB-20, LB-21, LB-4, LB-18, LB-13, LB-11, LB-26, LB-30, LB-31, LB-34, LB-35, and LB-40. Petrographic thin-sections were produced by Spectrum Petrographics (Vancouver, WA). Thin sections were mounted on standard 2″ by 3″ glass slides with 30 μm thickness. Slides were vacuum impregnated with clear epoxy resin. An Olympus BH-2 series polarizing light petrographic microscope with a circular rotatable stage and 4×, 10×, and 40× magnification power scope objectives was used to analyze thin-sections. Observations included assessments of sediment texture and lithology, sediment grains, authigenic minerals, sedimentary fabric, biogenic structures, and organic material following the terminology in Bullock et al. (1985). Matrix composition was quantified using visual estimates following Bullock et al. (1985). Thin-section photographs were taken using a Nikon Eclipse E400 POL microscope and scanned using a Prior OptiScanII Stage with an attached Nikon Eclipse Ci. The stratigraphic and petrographic descriptions and images (Supplement Figs. S1–S5) are used to define facies and depositional environments.

3.3. Diatoms

Thirty-six samples were processed using 30% H_2O_2 and 10% HCl to remove organic and carbonate materials, respectively. Processed material was evaporated onto coverslips, which were then mounted on slides using Naphrax. At least 300 valves were counted using the 100× magnification objective in samples where diatom valves were abundant. Samples with < 50 valves after five transects were considered as sparse diatom content and were removed from analysis. Species identifications were made using cosmopolitan floras (Krammer and Lange-Bertalot, 1986, 1988, 1991a, 1991b; Houk, 2003; Taylor et al., 2007) and regional floras (e.g. Rumrich et al., 2000; Maidana et al., 2011; Blanco et al., 2013).

Graphical and statistical analyses were performed using the *rioja* package on RStudio (Version 1.1.423) and C2 data analysis (Version 1.7.7). Diatom percent abundances were calculated and plotted with rare species (< 5%) omitted. Stratigraphically constrained cluster analysis (CONISS) was performed and evaluated for statistical significance using the broken stick model (Bennet, 1996).

3.4. Palynology

Approximately 20 g from 16 samples were separated for analysis at the U.S. Geological Survey in Reston, Virginia. One tablet of *Lycopodium clavatum* (batch number 938934) spores was added for calculating pollen concentrations. Sample preparation followed Faegri and Iversen (1989), Doher (1980), Traverse (2007), and Brown (2008); calcareous material was removed using HCl, and silicates were removed with HF;

processing continued by using acetolysis, KOH treatment, and sieving (150 μm - 5 μm mesh sizes). Slides were prepared with glycerin jelly, while the sample residue was kept in de-ionized water. Of all samples tested, LB-5, LB-6, LB-9, LB-10, LB-19, LB-21, LB-25, LV-29, LB-32, LB-33 and LB-39 contained sufficient pollen to count. To aid interpretation of Lauca Basin fossil floras, a surface sample taken from the mud-water interface in 29 m water depth from the nearby Lago Chungará (4515 masl) was also analyzed following the same procedure at the Senckenberg Research Institute and Natural History Museum Frankfurt. Before slides were prepared, the sample was further cleaned by using heavy liquid separation. One *Lycopodium clavatum* tablet (938934) was also added to compare pollen concentrations between the sub-recent and fossil palynological assemblage. At least 300 pollen grains were identified per sample. Identifications to the genus or family levels were performed through comparisons with pollen atlases (e.g. Heusser, 1971; Markgraf and D'Antoni, 1978; Roubik and Moreno, 1991), online databases (e.g. Bush and Weng, 2006), publications (e.g. Gosling et al., 2009; Palazzesi et al., 2012), and the tropical pollen reference collection of Frank E. Mayle (University of Reading/United Kingdom).

3.5. Stable isotope geochemistry

All samples containing calcium carbonate were dried and ground prior to analysis on a Finnigan-MAT 252 stable isotope ratio mass spectrometer coupled with a Kiel III carbonate preparation device in the Department of Geological Sciences at University of Florida. All oxygen isotopic results are expressed in standard delta notation relative to VPDB. Precision of the measurement (estimated based on analysis of NBS-19 standard measured along with the samples) 0.042‰ for $\delta^{18}O$ ($n = 8$). NBS-19 is defined as $\delta^{18}O = 2.2‰$ versus VPDB.

4. Results

4.1. Chronology

Maximum depositional ages were determined for samples LB-5 (1.68 m) and LB-36 (19.4 m) (Fig. 4). For sample LB-5, the 27 youngest grains provide a mean maximum depositional age of 5.57 ± 0.11 Ma (95% confidence interval). For sample LB-36 the 15 youngest grains yield a mean maximum depositional age of 5.44 ± 0.16 Ma (95% confidence interval). Both samples have age populations characteristic for ash deposits (in situ or very mildly reworked), with the majority of the grains forming the youngest age group for which the maximum depositional age was calculated. We assume that these youngest detrital zircons correspond to ages of regional volcanic activity. These new detrital zircon dates are similar to K/Ar dates (5.38 + 0.21 Ma and 6.20 + 0.24 Ma) determined on biotite separates from fallout ash layers in the Lauca Formation (dates attributed to C. Rundle and reported in Kött et al., 1995). Although the exact location of these latter samples is not given, the stratigraphic section of Gaupp et al. (1997) implies that they were from the lower part of Stage 2 sediments, likely in a similar stratigraphic position as our own. The new dates yield a mean sedimentation rate of 13.6 cm kyr^{-1} and a minimum sedimentation rate of 4.4 cm kyr^{-1}based on the maximum range of the age estimates. This sedimentation estimate comes from the maximum range of the age estimates, and, based on comparison with modern lacustrine sedimentation rates in the Altiplano (e.g. Fritz et al., 2007; Giralt et al., 2008; Cohen et al., 2015), we suspect the actual rate was likely an order of magnitude faster.

4.2. Sedimentology

4.2.1. Laminated mudstone (F1)

Lithofacies Fl is the most abundant lithofacies in the stratigraphic section (Fig. 5, see Supplementary Fig. S1). It consists of fine-grained clay and up to ~30% silt and sand grains (mainly plagioclase, oxidized biotite, olivine, and volcanic glass). The clay matrix displays unistrial birefringence under crossed polarizers in thin-section, meaning that individual layers show nearly continuous extinction due to uniformly oriented clay particles settled from suspension. Individual laminae in F1 are discontinuous and irregular, very thin to medium (0.005–4.0 mm thick), and range from planar parallel to convoluted, wavy, and non-parallel. An isolated occurrence of low angle cross bedding was observed possibly indicating the presence of current-ripples. Carbonate peloids and siliciclastic mud pellets are rare to common. Some thin sections have silt filled burrows or elongate lenses, and some contain siliciclastic mud pellets. Clusters of gypsum crystals that have been partially to fully replace by chalcedony are common. Lithofacies Fl reaction with dilute HCl in hand specimen varies from noncalcareous to strongly calcareous. The noncalcareous microfacies has sparse amounts of carbonate, excluding carbonate peloids, which were present throughout the section. The calcareous microfacies consists of variable amounts of micritic carbonate mixed with clay matrix. This microfacies contains very few ostracods or silicified algal structures. Iron oxide staining is present in all thin-sections, and, in some places, it is directly associated with weathered biotite grains.

4.2.2. Volcaniclastic mudstone (Fv)

Lithofacies Fv exists in four positions in the stratigraphic section at 2 m, 2.25 m, 19.4 m, and 21 m (Fig. 5, see Supplementary Fig. S2). This lithofacies can be subdivided into four microfacies: (1) ashy siltstone, (2) ashy mudstone, (3) ashy claystone, and (4) silty ash depending on the relative abundance of the siliciclastic matrix and volcaniclastic sediments. The matrix consists of a mixture of very fine-grained clay and silt (mainly plagioclase, oxidized biotite, olivine, glassy dacitic and rhyolitic volcanic rock fragments, and mica). The clay matrix displays unistrial birefringence. This lithofacies is typically massive. Laminae are very thin (0.05–0.5 mm thick), discontinuous, and irregular when present. Sediments in this lithofacies are noncalcareous to slightly calcareous. A few (5–15%) volcanic ash fragments appear to have been partially to fully alter to smectitic clay. Very few (< 5%) gypsum crystals are present. Staining by hydrous iron oxides is, in some places, directly associated with weathered biotite grains.

4.2.3. Carbonate (C)

Lithofacies C is most common throughout the middle of the stratigraphic section (~3–5 m), but it is also found in parts of the upper portion of the section (~15–17 m) (Fig. 5, see Supplementary Fig. S3). The matrix consists of carbonate and clay minerals, and it also contains frequent (5–30%) gypsum crystals. Carbonate (dominantly micrite with very minor microspar) makes up > 50% of all thin-sections. In some samples, there are very thin (0.05–0.5 mm thick) laminae of sandy clay that display unistrial birefringence. Carbonate peloids appear throughout, as do some small opaque fragments that may be organic matter. Dissolved ostracod voids filled with calcite are present. Staining by hydrous iron oxides is, in some places, directly associated with weathered biotite grains.

4.2.4. Evaporite (E)

Lithofacies E is present near the middle of the stratigraphic section (~3–7 m) (Fig. 5, see Supplementary Fig. S4). The matrix consists of carbonate and clay minerals with clay, silt, and sand-size grains. Hand samples are typically non-fissile. Silt and sand grains consist of plagioclase, biotite, olivine, hornblende, and volcanic ash and glassy volcanic rock fragments. Lithofacies E can be subdivided into two microfacies: (1) gypsum and carbonate, and (2) gypsum and clay. The gypsum and carbonate microfacies has a micrite matrix with a minor component of clay. Gypsum abundance varies from 40 to 100%. In some thin-sections, crystalline gypsum is nearly pure and forms coalescent ingrown crystals. Elsewhere, gypsum crystals exist as discrete laminae, convoluted laminae, or discontinuous non-parallel laminae. Carbonate peloids and ooids are present, but organic material is absent.

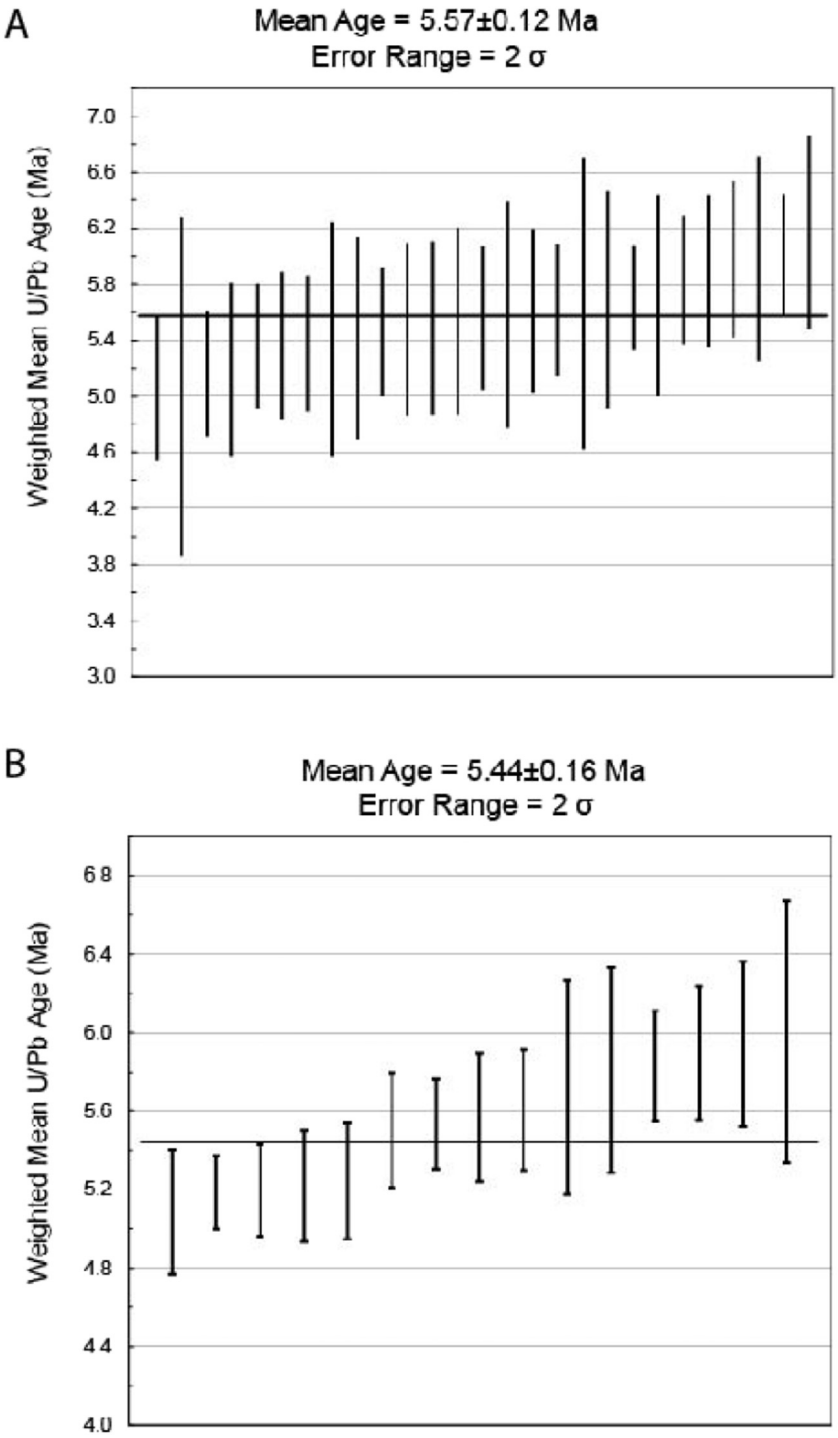

Fig. 4. Results of zircon dating for samples near the top (A: LB-36, 19.4 m) and the base (B: LB-5, 1.68 m) of the Lauca Basin outcrop. The samples are arrayed along the x-axis based on ascending age.

The gypsum and clay microfacies has a dominant (50–70%) clay matrix with minor silt and sand. Laminae are generally discontinuous and irregular and vary in thickness between samples (0.05–3.0 mm). In many cases, carbonate peloids are compacted, with primary porosity filled by lenticular authigenic gypsum crystals. Rare carbonate peloids and possible filled burrows or elongate lenses are present, as well as small opaque fragments that may be organic matter. Ostracod carapaces (*Heterocypris incrongruens*) filled with calcite spar are present. Iron oxide staining is present in some places, where it is directly associated with weathered biotite grains.

4.2.5. Muddy sandstone (SF)

Lithofacies SF is one of the least abundant lithofacies (Fig. 5, see Supplementary Fig. S5). It can be subdivided into two microfacies: (1) massive and (2) laminated. The massive microfacies was examined in one sample (1.68 m) (Fig. 5). It consists of massive, poorly sorted sand grains in a muddy matrix. The laminated microfacies was examined in three samples (3.8 m, 17.4 m, and 22.5 m) (Fig. 5). This lithofacies is characterized by frequent (15–30%) discontinuous and irregular laminae. Intact, very thin (0.025–0.2 mm thick), horizontal to sub-horizontal laminae of mica grains are prevalent. The matrix consists of mud, with silt and fine to coarse-grained sand. Sediment grains include

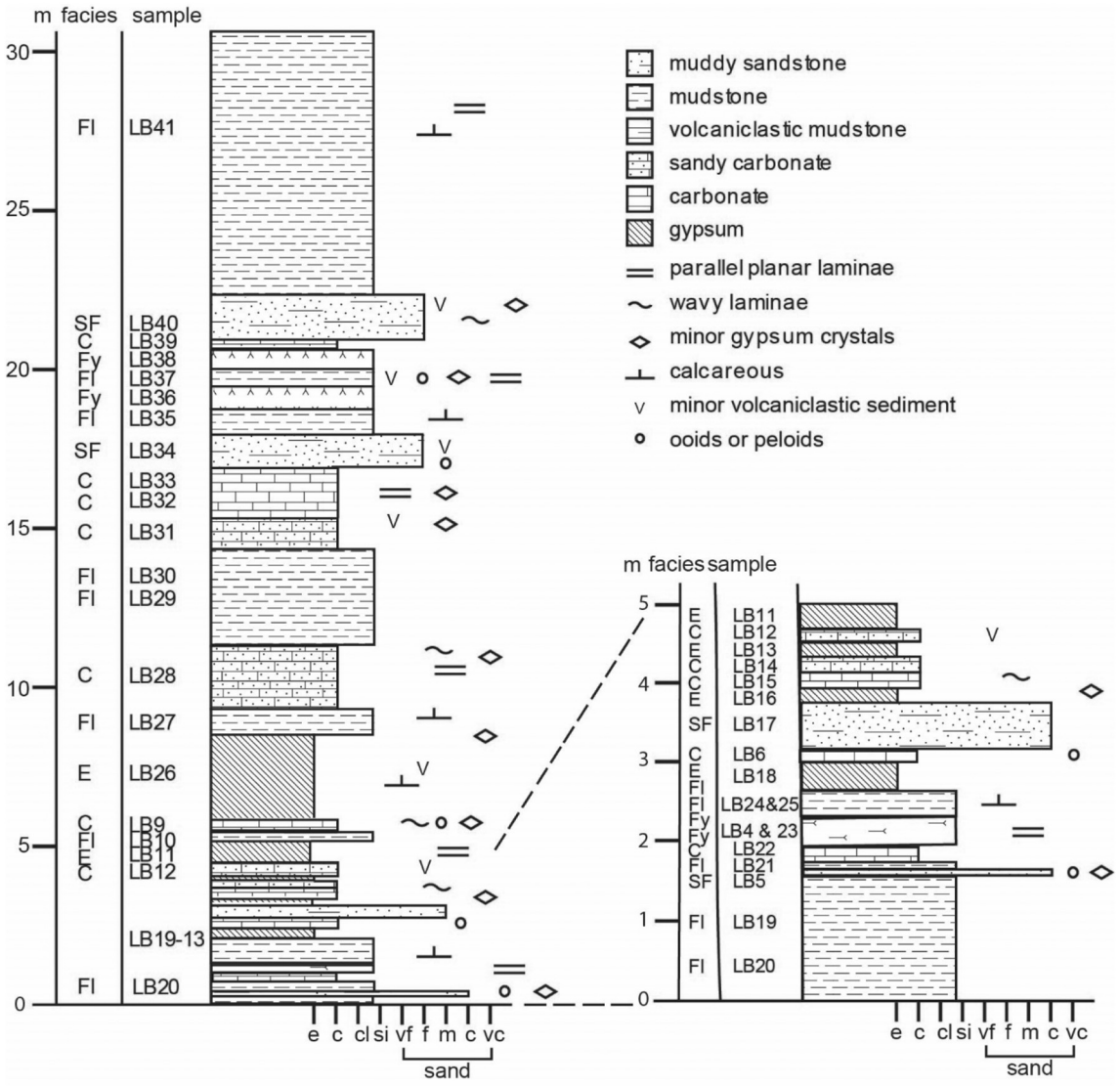

Fig. 5. Stratigraphic column of the Lauca Basin outcrop (panel C in Fig. 2) (left) and a detailed view of the outcrop base (0–5 m) (right).

dominantly (50–70%) very fine to fine sand consisting of plagioclase, sanidine, biotite and micaceous material, ferromagnesian silicate minerals (olivine, augite), volcanic ash, and glassy volcanic rock fragments (2–10% of the overall composition). Sand grains are euhedral to subhedral, and they are subrounded to subangular. Many clusters of gypsum crystals are partially to fully replace by chalcedony. Individual crystals are lenticular tabular forms and are subhedral to euhedral. Sediments in this lithofacies are noncalcareous to slightly calcareous. Rare carbonate peloids and possible filled burrows are present. Iron-oxide staining is, in some places, directly associated with weathered biotite grains.

4.3. Diatoms

Thirty-one genera and 74 species were identified in the Lauca Formation (see Supplementary Table S1 and Figs. S6–S9). Thirty of the 36 samples contained sufficient concentrations of diatoms for valve counts. Diatoms were either absent or very sparse at 1.68 m, 17.4 m, 19.4 m, 21 m, 22.5 m, and 31 m. Samples generally exhibit poor preservation, indicating that dissolution of diatom valves is significant in the Lauca Formation sediment.

Benthic, hypo- to hypersaline, and alkaline tolerant species dominate the Lauca paleolake record, with tychoplanktic and planktic species as minor components (Figs. 6; 8). Three benthic species account for > 40% of the diatoms recorded: *Navicula salinicola*, *Halamphora coffeaeformis*, and *Navicula pseudogracilis* var. 1. Secondary components (> 5%) of the benthic flora include *Halamphora acutiuscula*, *Halamphora* c.f. *luciae*, *Navicula* cf. *cryptocephala*, *Navicula erifuga*, *Navicula* cf. *pseudogracilis* var. 2, *Navicula tenelloides*, *Nitzschia* cf. *bacillum*, *Nitzschia valdecostata*, *Planothidium lanceolatum*, *Rhopalodia acuminata*, and *Staurophora soodensis*. Tychoplanktic species increase in abundance from 3.95 to 5.7 m and mainly consist of small fragilarioid species, including *Pseudostaurosira polonica*, *Staurosirella leptostauron* var. *dubia*, *Staurosirella salitre*, and *Staurosirella* cf. *pinnata*. Planktic diatoms are rare but are most abundant at the base of the outcrop. Planktic cyclotelloid species, including *Cyclotella* cf. *glomerata* and large valves of *Discostella* cf. *stelligera*, dominate the record at 2.25 m and are minor components in samples below and above at 2 m and 2.43 m, respectively. Members of the *Aulacoseira distans* complex are found in low abundance from 2.25 to 5.7 m.

Three diatom zones are designated through hierarchically constrained cluster analysis (CONISS) and the broken-stick model. Zones LBDZ-1 and LBDZ-3 are subsequently divided into subzones LBDZ-1A-1C and LBDZ-3A-3C on the basis of qualitative observations (Fig. 6).

Zone LBDZ-1A (0–2 m) is characterized by co-dominance of the meso- to hypersaline and alkaline taxa *N. salinicola* and *H. coffeaeformis*,

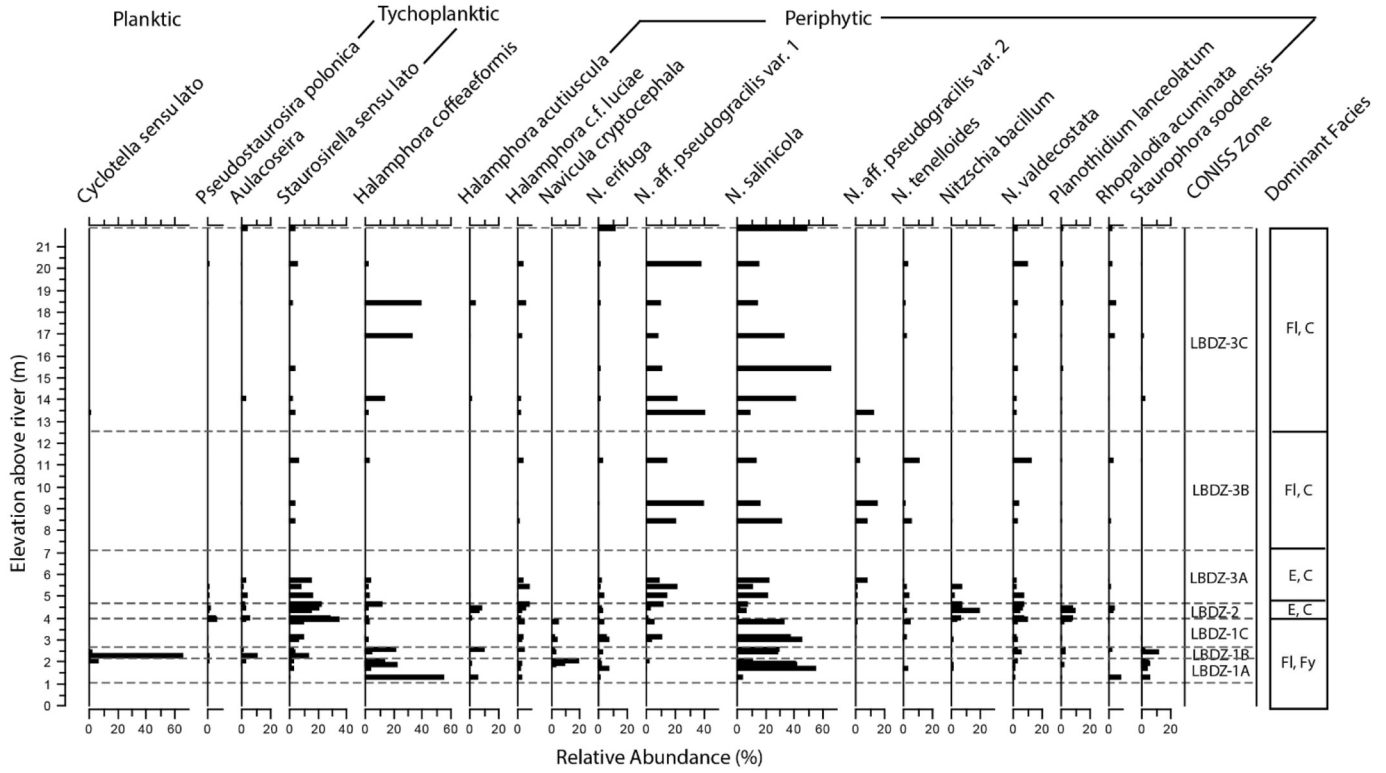

Fig. 6. Diatom assemblage stratigraphy for the Lauca Basin presented as relative abundance (% of the total valve count). Only diatom species with > 5% abundance are plotted. CONISS diatom zones are shown, along with the associated numerically dominant facies.

and hypersaline *Staurophora soodensis*. The cosmopolitan species *N. cryptocephala* is also observed.

Zone LBDZ-1B (2.25 m) consists of a single sample and is dominated by the planktic species *C.* cf. *glomerata* and *D.* cf. *stelligera*, characteristic of moderate water depths and a range of salinities. Tychoplanktic *Staurosirella* and *Aulacoseira* species are also present.

Zone LBDZ-1C (2.43–3.8 m) exhibits decreases in *H. coffeaeformis*, *N. cryptocephala*, and *S. soodensis* with subsequent increases in *N. salinicola* and *N. pseudogracilis* var. 1, as well as the tychoplanktic taxon *S.* cf. *pinnata*. Overall taxonomic richness decreases, and valves are very poorly preserved. This shift is contemporaneous with a decrease in planktic species.

Zone LBDZ-2 (3.95–4.45 m) shows increases in nitzschioid and tychoplanktic taxa. Within the benthic flora, *N. salinicola* and associated naviculoid taxa decrease to their lowest abundance in the stratigraphic sequence. This is offset by increases in *Nitzschia bacillum*, *Nitzschia valdecostata*, *P. lanceolatum*, and *Tryblionella hungarica*. This shift in benthic species is coincident with an increase in small fragilarioid tychoplanktic species, mainly including *P. polonica* and *S.* cf. *pinnata*. Valves from the planktic *A. distans* complex are also present. Aerophytic species from the genera *Luticola* and *Pinnularia* are more common than in other portions of the outcrop.

Zone LBDZ-3 is divided into three subzones LBDZ-3A, LBDZ-3B, and LBDZ-3C. All three of these zones are characterized by a return to naviculoid dominance, with the highest abundances observed in *N. salinicola* and *N. pseudogracilis* var. 1. The first subzone LBDZ-3A (4.6–5.7 m) has relatively high taxonomic richness, low abundances of tychoplanktic fragilarioid species, and an abundance of nitzschioid taxa. Similar to Zone LBDZ-2, *Aulacoseira* valves occur in low abundance in nearly all samples.

Subzone LBDZ-3B (8.4–13.4 m) has complete naviculoid dominance, similar to that observed in Zone LBDZ-1B. While subzone LBDZ-3C (14–21.8 m) contains shifts in dominance between *N. salinicola*, *N. pseudogracilis* var. 1 and var. 2, and *H. coffeaeformis*. All three of these species are meso- to hypersaline and prefer alkaline waters.

4.4. Palynology

The fossil pollen assemblages of the Lauca Basin are diverse, with > 100 different taxa among > 70 plant families. With the exception of samples from 1.83 m, 2.55 m, and 13.4 m, fern spores are rare and comprise < 10% of the whole pollen and spore assemblage (Fig. 7), with no correlation to pollen concentration (pollen and spores per gram dry sediment). Pollen concentrations are highly variable, with some samples containing < 1000 pollen grains per gram (1.68 m; 3.1 m; 21.8 m), and others with > 3000 (16.9 m) and > 5000 (1.66 m) pollen grains per gram (Fig. 7). A step-wise decrease in pollen content is recorded between 1.66 m and 1.68 m, where the pollen concentrations decrease up section from > 5000 grains per gram to ~500, despite continued high diversity. Most of the pollen and spore counts are pollen grains (77.9% to 97.6%) of herbs and shrubs (39.1% to 77.3%), whereas tree taxa only exceed 10% toward the top of the section (see Supplementary Table S2). The most common taxa in all samples are Poaceae (12.9% to 28.6%), followed by *Acaena/Polylepis* (7.5% to 29.4%), *Podocarpus* (1.6% to 16.4%), Asteraceae (5.5 to 16.2% excluding *Franseria/Ambrosia*), and Vivianaceae (1.7% to 9.6%). Overall, Poaceae, *Acaena/Polylepis*, and the Asteraceae *Franseria/Ambrosia* increase toward the top of the section, resulting in a concomitant decrease in species diversity. The algae *Pediastrum* and *Botryococcus* were both present in all samples, although they were not included in the palynological calculations.

In contrast, the modern sample from nearby Lake Chungará (see Fig. 2A) contains a higher percentage of Poaceae (28.9%) and Asteraceae (28.6%) and almost no fern spores (0.75%). Other important components of the sample are *Acaena/Polylepis* (4.5%), henopodioideae (4.5%), *Franseria/Ambrosia* (6.5%), and *Myriophyllum* (12.7%), with low percentages of arboreal pollen grains (1.5%).

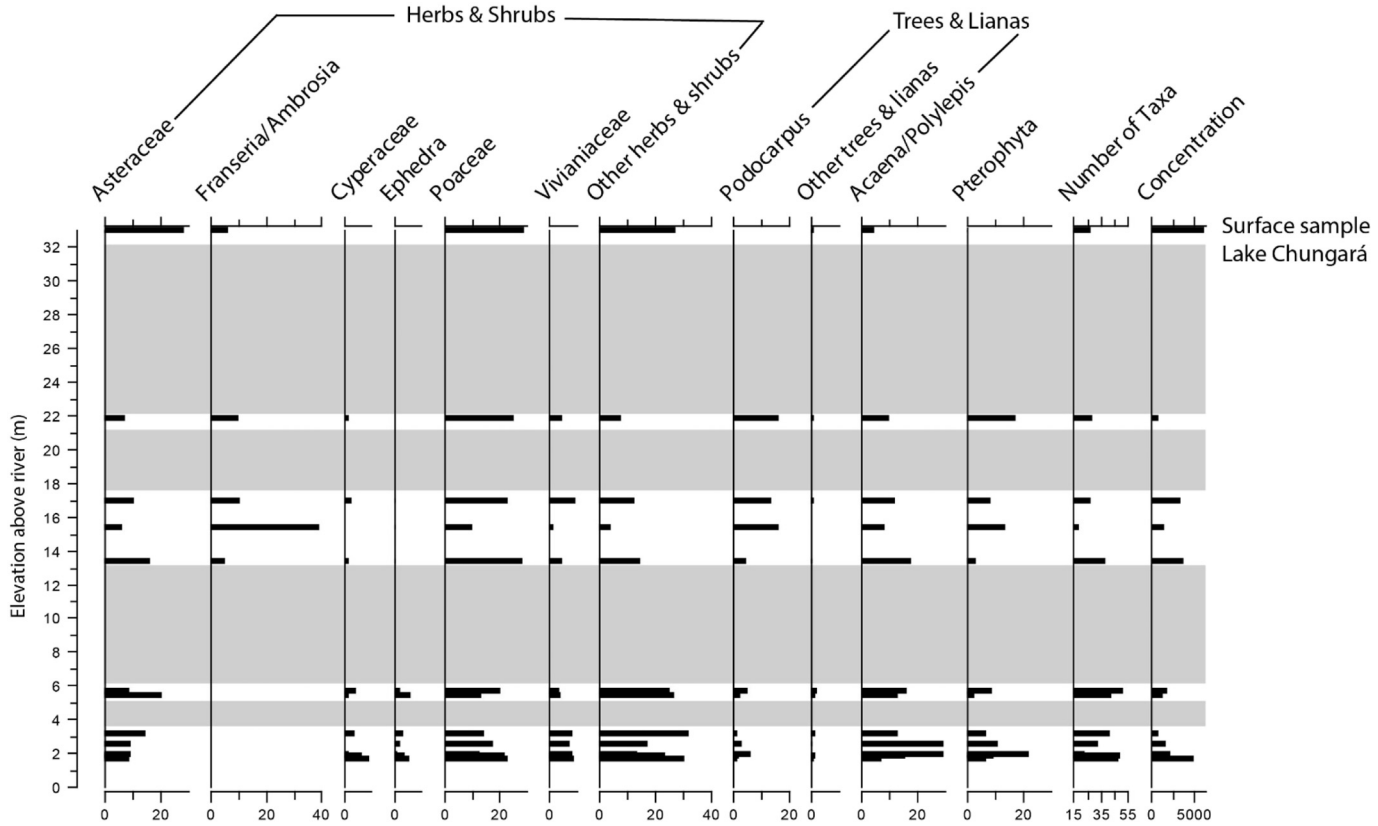

Fig. 7. Pollen assemblage stratigraphy for the Lauca Basin presented as abundance (% of the total). Only pollen groups with significant abundance are plotted. Gray shaded areas indicate gaps in pollen sampling.

4.5. Stable isotope geochemistry

All carbonate-bearing samples were analyzed for stable oxygen isotopes. The $\delta^{18}O$ values range from −8.96 to −2.22‰, with a mean value of −6.19‰. Values of $\delta^{18}O$ undergo several oscillations of ca. 5 to 6‰ in the stratigraphic sequence (Fig. 8). Most of these oscillations have single point maxima or minima indicative of an under-sampling bias.

5. Discussion

5.1. Paleoenvironmental history of the Lauca Basin

Radiometric dating of detrital zircons from the Lauca Basin outcrop yields maximum depositional ages of ~5.57 Ma and ~5.44 Ma. During this time, the Altiplano had most likely already reached its modern altitude (> 4500 masl) (Garzione et al., 2006, 2014; Ghosh et al., 2006; Poulsen et al., 2010). Multiple volcaniclastic beds occur throughout the sequence, which suggest near-continuous volcanic activity in the region, contemporaneous with sedimentation in the basin.

5.1.1. Lacustrine setting

The interpretations of the paleo-lacustrine sequence (Fig. 8) of the Lauca Basin presented here are consistent with previous paleoenvironmental reconstructions (Kött et al., 1995; Gaupp et al., 1999) and contribute new data suggesting that the lake was highly dynamic during the Miocene-Pliocene transition. Multiple proxies, including the relatively enriched $\delta^{18}O$ values, suggest that the lake basin was closed during deposition of most of the sequence. Outcrop samples contain the filled voids of an ostracod, *Heterocypris incongruens*, a species typically found in shallow, temporary pools, ephemeral springs, shallow streams, or weedy littoral zones, supporting the inference of a generally shallow lake (Smith and Horne, 2016). The diatom record mainly consists of species adapted to high salinities, shallow water depths, and alkaline waters. Diatom zones correspond to shifts in salinity likely driven by changing lake level (see Fritz, 2013 for a review) and further support the inference that the Lauca paleolake was closed.

The early paleolake environment is dominated by laminated mudstone facies (Fl, Fv) (Figs. 5, 8). The laminated mudstone likely indicates deeper water, an inference that is supported by the observed diatom assemblage. The co-dominance of hyposaline, mesosaline, and hypersaline taxa suggest an early lake of moderate depth, with significant temporal fluctuations in lake level. CONISS Zone LBDZ-1A contains the species, *S. soodensis*, reported to be tolerant of hypersaline conditions and periodic desiccation and found contemporaneous with hyposaline taxa in Lake Oloidien (Cocquyt, 2004). Similar conditions of seasonal variation in water level in the Lauca paleolake may have occurred at this time. Alternatively, habitat juxtaposition cannot be disregarded, because the development of a freshwater surface-layer over a more saline layer is quite common in saline waterbodies (Gasse et al., 1987).

Samples from the overlying subzone LBDZ-1B contain planktic diatoms in higher abundance than other portions of the section (Fig. 8). Progradational geometries from lacustrine deltaic sediments indicate that high-stand water depths were likely < 5 m (Gaupp et al., 1999). In general, planktic diatom abundance in the section is low, and planktic taxa were observed only in the lowermost portion of the outcrop, accounting for < 20% of the assemblage, perhaps indicative of water depths < 10 m (Wang et al., 2012). Together, these records imply that between ~5.57 to 5.44 Ma the Lauca paleolake was always relatively shallow, but with the deepest lake conditions at the base.

The stratigraphic interval from 3 to 5 m (Fig. 5) shifts from mudstone dominant (Fl) to one dominated by carbonate (C) and evaporite (E) facies that lack laminations, which suggests an overall shallower,

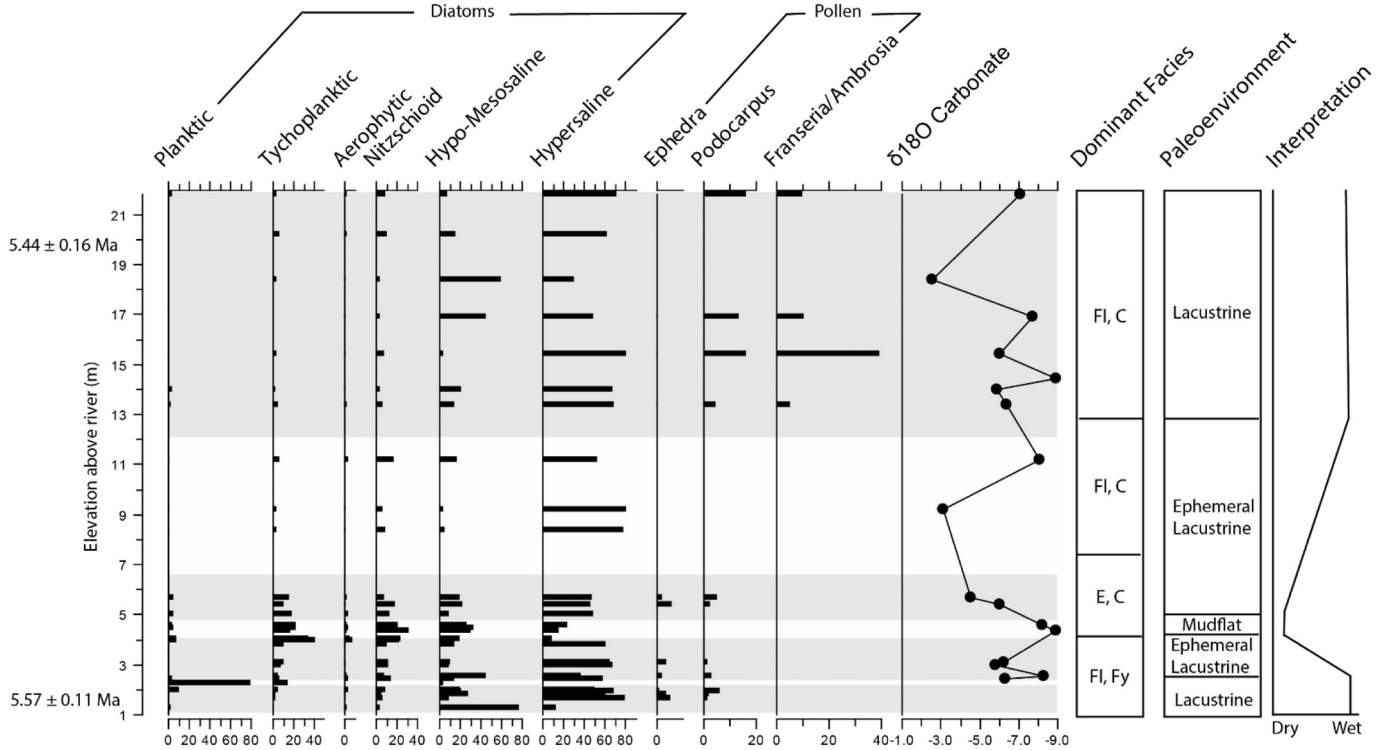

Fig. 8. Summary figure of the Lauca Basin proxy data including diatom ecological groups and important pollen groups plotted as percent abundance, oxygen isotopic composition of authigenic carbonates (‰), the numerically dominant lithofacies compared to CONISS diatom zones (differentiated by gray and white shading, see Fig. 6 for reference), the inferred paleoenvironments, and the interpreted paleoclimate (dry/wet).

well-oxygenated lake that varied in depth through time. Two diatom zones (LBDZ-1C and LBDZ-2) coincide with the change in lithology. In diatom zone LBDZ-1C, taxonomic richness is low, preservation is poor, and naviculoid species dominate. Commonly, taxonomic richness is inversely correlated with salinity (Hammer, 1986; Hammer et al., 1983, 1990; Fritz et al., 2010), and dominance of naviculoid taxa is typical of high-elevation lakes and wetlands in the Andes (Maidana et al., 2011). Zone LBDZ-2 represents a shift to an assemblage dominated by tychoplanktic and nitzschioid species. Tychoplanktic species include members of the *A. distans* complex and small *Staurosirella* species that thrive in well-mixed shallow waters. Members of the *A. distans* complex are commonly reported from shallow lake to wetland environments. The evaporitic facies imply a shallow lake, wetland, or ephemeral mudflat conditions. The lower diversity combined with the dominance of tychoplanktic species suggests that there was a step-wise decrease in lake-level.

The remainder of the section above 5 m in stratigraphic height (Fig. 5) mainly consists of laminated mudstone (Fl) and carbonate (C) facies with intercalated minor muddy sandstone (SF) and volcaniclastic mudstone (Fv). The paucity of evaporite facies suggests a return to a more stable lake of moderate depth. Nevertheless, lake level is still likely to have fluctuated, as indicated by shifts in diatom assemblages. Diatom zone LBDZ-3A is taxonomically rich and dominated by hyposaline to mesosaline species, implying lake-level rise and a subsequent freshening of the lake. This zone has the highest taxonomic richness in the outcrop, suggesting a diversification of lake habitats associated with the return to deeper water. Alternatively, the coincidence of diatom species with a large range in their ecological spectra could indicate highly variable short-term fluctuations in the precipitation-evaporation ratio. Diatom zone LBDZ-3B mirrors conditions in zone LBDZ-1C exhibiting naviculoid dominance, which suggests that the lake was relatively shallow and saline. From ~13.5 m to the top (LBDZ-3C), the dominant diatoms vary between *H. coffeaeformis*, *N. salinicola*, and *N. pseudogracilis* var. 1. In other regional lakes, *H. coffeaeformis* has been observed in Mg-rich waters with a salinity optimum of 18.73 g L^{-1}, whereas *N. salinicola* has a salinity optimum of 90.92 g L^{-1} (Sylvestre et al., 2001). *N. pseudogracilis* was reported in highly saline waterbodies from wetlands in Argentina (Maidana et al., 2011). Thus, these intervals suggest increased salinity and/or changes in ionic composition.

Muddy sandstone and volcaniclastic mudstone facies at 17.4 m, 19.4 m, 21 m, and 22.5 m (Fig. 5) are either devoid of diatoms or contain diatoms in very low abundance suggesting either inhospitable conditions for diatoms to live, or higher rates of diatom valve dissolution. Muddy sandstones may record a shallow lake or ephemeral mudflat conditions. The absence of diatoms in these muddy sandstone samples implies that the depositional environment may have been too shallow to preserve a diatom assemblage. By contrast, the volcaniclastic mudstone, although containing a low abundance of diatoms, contains a proportionally higher abundance of planktic species in some samples. Thus, the volcaniclastic mudstone may reflect deeper lake conditions with varying degrees of preservation.

Several different processes are possible controls on the oxygen isotopic value of the lacustrine carbonate units. (1) Elevation exerts the strongest control on $\delta^{18}O$ of precipitation ($\delta^{18}O_p$) in the tropical Andes and Altiplano (Fiorella et al., 2015). Thus, the $\delta^{18}O_p$ of local precipitation is far more negative than precipitation that falls along the atmospheric trajectory of water vapor from its Atlantic source region across the lowland Amazon (Rozanski and Araguás, 1995). In addition, uplift is responsible for a Cenozoic decrease in the isotopic composition of Altiplano precipitation. Garzione et al. (2006) observed a decrease of $\delta^{18}O$ of lacustrine and soil carbonates from the western Altiplano of Bolivia from values averaging −11‰ at 11 Ma to ~−14‰ at 6 to 7 Ma and attributed this decrease to rapid uplift between 10.3 and 6.7 Ma (Ghosh et al., 2006). Given that their study area is nearby and tectonically comparable to the Lauca sedimentary sequence, it is likely that our study area had obtained its present-day elevation by the time of deposition of the Lauca strata. (2) The precipitation-weighted annual value of $\delta^{18}O_p$ on the Altiplano of Bolivia and Chile between 18°S and

21°S has large spatial and inter-annual variability as a result of both remote and local meteorological influences (Aravena et al., 1999; Fiorella et al., 2015). (3) Global climate variability can bring about large local changes in $\delta^{18}O_p$ associated with glacial-interglacial cycles (Thompson et al., 1998), as well as remote climate influences, such as changing Cenozoic atmospheric CO_2 levels, increasing width of the Atlantic Ocean (Liu et al., in review), and possible Pliocene onset of Pacific Walker circulation (Poulsen and Jeffrey, 2011). In general, wetter conditions related to an intensified SASM (Baker and Fritz, 2015) decreased $\delta^{18}O_p$. (4) Major changes in the isotopic composition of water and the resultant $\delta^{18}O$ of precipitated calcite ($\delta^{18}O_c$) takes place as a result of variability in relative humidity and evaporation/precipitation ratios (Fontes et al., 1979; Gonfiantini et al., 2002; Baker et al., 2009). (5) Because the isotopic fractionation between calcite and water is temperature dependent, the isotopic composition of the solid carbonate phase, $\delta^{18}O_c$, may vary due to environmental temperature, itself a function of several factors including changing elevation, global climate change, and changing environment of deposition. (6) Finally, although diagenesis could potentially alter their original oxygen isotopic values, the Lauca Basin succession is weakly consolidated, was never been deeply buried, and petrographic observations provide no indication of substantive diagenesis.

The preceding discussion indicates that the Lauca Basin is a highly under-constrained geochemical system. Nonetheless, the observed range of values of $\delta^{18}O$ is large. Because these sediments have experienced minimal diagenesis, their isotopic values are related to those of environmental water during or near the time of deposition. Assuming that ancient lacustrine carbonate sediment precipitated at temperatures near the modern annual average air temperature (ca. 6 °C), the isotopic values of their source lake waters can be calculated (O'Neil et al., 1969) to range from −3.5 to −10.7‰ SMOW, considerably higher than the unknown, but likely, mean annual value of $\delta^{18}O_p$ ca. −16‰ SMOW.

If the Lauca paleolake was always closed, then an isotopic value of ca. −3.5‰ SMOW would be predicted for isotopic and hydrologic equilibrium at Altiplano humidity levels (Gat, 1995). More negative isotopic compositions of lake water in a closed-basin lake could be produced during non-steady-state hydrologic conditions, such as during seasonal or longer-term filling of the lake. Alternatively, if the lake was not always closed, then more negative isotopic values could represent a higher fraction of throughflow relative to evaporative loss.

The relatively depleted values observed in the lower part of the section (2.5 to 5 m) coincide with relatively deep conditions deduced from diatom assemblages (Figs. 5, 8). It may be that paleolake Lauca was overflowing at this time. The second large negative isotopic excursion (11.2 to 16.9 m) corresponds to a shallow, hypersaline lacustrine period, and the isotopic excursions may result from periods of desiccation followed by filling. Alternatively, or additionally, these isotopic excursions may represent shifts in precipitation and its isotopic composition. In the absence of additional data, both of these hypotheses remain viable.

5.1.2. Terrestrial paleoenvironments

The vegetation around the Lauca paleolake shows similarities to, and differences from, the modern surface pollen samples from Lake Chungará (4515 masl). The magnitude of long-distance transport from lower elevations is surely small but could include a substantive contribution of *Alnus*, *Podocarpus*, Polypodiaceae, and *Cissus*, which were identified as single grains (Reese and Liu, 2005; Kuentz et al., 2007).

The modern surface sample from Lake Chungará is dominated by Poaceae and Asteraceae, which are typical of modern high-elevation grassland (puna vegetation) of the surrounding region (Rundel and Palma, 2000; Lambrinos et al., 2006). Vegetation typical of nearby wetlands, including *Myriophyllum*, Juncaeae, and *Plantago* (Rundel and Palma, 2000; Reese and Liu, 2005; Ortuño et al., 2011) was also detected in the Chungará surface sample.

The fossil samples from the Lauca Basin section are also characterized by a high abundance of Poaceae and, to a lesser extent, Asteraceae, with a higher diversity in the fossil samples than modern. We interpret high abundances of several taxa as representing local vegetation, including *Podocarpus*, *Kageneckia*, and *Ephedra*; likewise, the rare but constant presence of Bignoniaceae, Bromeliaceae, *Cissus*, Convovulaceae, Ericaceae, and Urtricaceae/Moraceae indicates their local presence. These taxa are absent from the modern Lauca Basin, rather, they occur in seasonal/cloud forests at lower elevations and with higher precipitation in Bolivia and southern Peru (Reese and Liu, 2005; Kuentz et al., 2007; Ortuño et al., 2011). Although Vivianaceae, mostly represented by *Balbisia*, is absent on the Altiplano today, it is abundant in fossil assemblages. *Balbisia* is known from a wide range of environments, including arid to semi-arid climates in the Andes and Atacama Desert (Palazzesi et al., 2012).

Another important element of the Miocene-Pliocene assemblage is *Acaena/Polylepis* (Figs. 5, 6). Multiple species of *Polylepis*, a shrub or tree, are present in the region at high elevations up to 4900 m (Rundel and Palma, 2000), but their pollen cannot be distinguished in the light microscope from *Acaena*, an herb known from the warm, humid valleys of Bolivia (Ortuño et al., 2011). Because of the high abundance of *Acaena/Polylepis* grains and the close similarity of the Lauca paleovegetation to drier habitats of the Altiplano today, we hypothesize that the grains are more likely assignable to *Polylepis* rather than *Acaena*. The oldest fossil *Polylepis* occurrence pre-dates the Lauca Basin section in the Late Miocene (10.66 ± 0.06 Ma) (Berry, 1922; Gregory-Wodzicki et al., 1998).

The latest Miocene pollen record from the Lauca Basin strongly suggests a terrestrial setting with more closed vegetation than present, characterized by the occurrence of seasonal forests and open grassland and shrubland, resembling a transitional stage between shrubby grassland and seasonal rainforest/cloud forest. Temporal variations in the pollen assemblage, however, probably reflect shifts in temperature and moisture balance. For example, decreased abundance of *Ephedra*, greater abundance of *Podocarpus*, and the appearance of *Franseria/Ambrosia* up-section may reflect a shift from fluctuating and possibly drier conditions to wetter conditions (but still presumably semi-arid), favoring the expansion of tree species and other species of sub-puna vegetation today. Variations in the lowermost 5 m of the section are most likely linked to preservation, which may be used as an indicator of unstable conditions (Fig. 7).

5.2. Paleoclimatic implications

Paleolake records in high-elevation regions can be influenced by tectonic, volcanic, and climatic factors. The presence of the high-altitude taxon, *Polylepis*, in the Lauca paleolake indicates that the basin had likely already reached its current elevation by the time of sedimentation. The pollen and diatom records indicate a variably arid to semi-arid climate over this interval (Fig. 8). The base of the outcrop is characterized by relatively deep lacustrine conditions, which may have resulted from a generally “wetter” climate, coupled with temporally drier intervals that supported *Ephedra* colonization and both hypo- to hypersaline diatom species. Therefore, we interpret progressive aridification from 2.43 to 4.45 m in the stratigraphic column (Figs. 7, 8). Decreases in wetland vegetation during this time support either a decrease in precipitation, an increase in evaporation, or both. The remainder of the record is characterized by a return to deeper lacustrine conditions, punctuated by shifts in the diatom assemblage between meso- to hyper-saline dominant species, implying changes in annual precipitation over time.

5.3. Regional context

Records of Miocene-Pliocene lacustrine sequences from the northern central Andes on the Altiplano are sparse (Fig. 1). The available records are mainly from the central Andes, including the Quillagua-Llamara

Basin in the Central Depression (Sáez et al., 1999), the Calama Basin (May et al., 1999; de Wet et al., 2015; de Wet et al., in review), the Salar Grande (Chong et al., 1999), and the Tiliviche paleolake (Kirk-Lawlor et al., 2013). Studies of Miocene-Pliocene lake sediments from the Altiplano are limited to outcrops from the Descanso Formation in the Descanso-Yaurí Basin (Vélez et al., 2017). Thus, data from the Lauca Basin fill a gap in regional paleoenvironmental and paleoclimatic comparison.

To the north, the slightly younger Pliocene Descanso Formation consists of diatomaceous lacustrine and marsh/wetland deposits (Vélez et al., 2017). Both the Lauca Formation and the Descanso Formation sedimentary records imply high temporal variability, with wet periods that allowed for small populations of planktic diatoms and hyposaline tolerant species, and dry periods producing times of elevated salinity or dessication allowing for colonization of hypersaline diatom species. To the south, the Opache Formation (ca. 3.5 Ma),the Quillagua-Llamara Formation (~6 Ma), and the Tiliviche paleolake (6.4 Ma) record shifts between variably saline lacustrine and palustrine conditions (Sáez et al., 1999, 2012; Kirk-Lawlor et al., 2013; de Wet et al., 2015). These facies were interpreted as climatically driven and are consistent with wetter-than-modern climate. Thus, most regional studies from the Altiplano and the Central Andes, including the present study, suggest a wetter than present climate at the onset of the Miocene-Pliocene transition. The widespread variability in the hydrological balance supports the conclusion that regional climate was also highly variable.

Globally, the late Miocene to early Pliocene is characterized by higher-than-modern atmospheric CO_2, higher temperatures, a decrease in meridional and latitudinal SST gradients, and absence of Arctic sea ice (Fedorov et al., 2006, 2013). An enhanced SASM, perhaps resulting from higher-than-modern CO_2 levels or other changes that affected the teleconnection of the SASM with the North Atlantic region (Baker and Fritz, 2015), may have been responsible for the somewhat higher precipitation on the Altiplano, as well as seasonal climatic conditions (Labraga, 1997; Rada et al., 1997; Vélez et al., 2017).

In this part of the Central Andes, variability in the water balance could also conceivably be related to variation in the intensity of cold oceanic currents in the Pacific (Sáez et al., 1999, 2012). Warming of coastal sea-surface temperatures due to decreased coastal upwelling during El Niño conditions can decrease the low-level inversion along the Pacific coast (de Wet et al., 2015), leading to increased Pacific derived. Just how far inland and how high altitude this precipitation could reach is a matter of conjecture. We favor the explanation that it was an intensified SASM that was responsible for the wetter-than-modern climate conditions during Lauca sedimentation given its prominent influence on precipitation amount in contemporary and Pleistocene times.

6. Conclusions

The Chilean Altiplano near the Miocene-Pliocene boundary had likely attained its modern elevation but was a landscape substantially different from that of today. Detailed multi-proxy analysis of paleo-lake sediments from an outcrop in the Lauca Basin of northern Chile provided an opportunity to evaluate ecosystem response to changes at the Miocene-Pliocene boundary. New radiometric dating of detrital zircons in volcanic tuffs near the base and top of the sequence, respectively, yielded maximum depositional ages of ~5.57 Ma and ~5.44 Ma. Successions of mudstones, carbonates, and evaporites, coupled with shifts in the diatom assemblage and in $\delta^{18}O$ values, suggest deposition in a closed or nearly-closed basin that fluctuated in level and was variably saline and alkaline in response to temporal variation in precipitation. The data suggest that the paleolake was deepest near the base of the sequence, with shallow to moderate lake levels above. The pollen assemblage is typical of sub-puna vegetation with a higher proportion of forest pollen than modern. These changes in inferred lake-level and vegetation were related to changes in precipitation-evaporation balance, likely driven by changes in the intensity of the SASM. Overall, these observations suggest a regional climate that was arid to semi-arid, seasonal, and wetter than today. Our data agree with other regional sedimentological records documenting highly variable precipitation across the Miocene-Pliocene transition.

Acknowledgements

Supported by NSF EAR-1338694 and NSF EAR-1251678 to Sherilyn Fritz and Paul Baker. Supported by FAPESP fellowship project 2014/05582-0 and the FAPESP BIOTA/NSF-Dimensions project 2012/50260-6 to Andrea Kern for pollen analysis. Supported by US Geological Survey Climate Research & Development Program. Thanks to John Barron, Lynn Wingard, and two anonymous reviewers for thoughtful comments and contribution to figures and discussion on an earlier version of the manuscript. Thanks to Les Howard (School of Natural Resources, University of Nebraska-Lincoln), who assisted with GIS graphics, and Alison Smith who identified the ostracod casts.

Appendix A. Supplementary data

Supplementary data to this article can be found online at https://doi.org/10.1016/j.palaeo.2019.109336.

References

Aravena, R., Suzuki, O., Peña, H., Pollastri, A., Fuenzalida, H., Grilli, A., 1999. Isotopic composition and origin of the precipitation in Northern Chile. Appl. Geochem. 14, 411–422.

Arroyo, M.T., Squeo, F.A., Armesto, J.J., Villagran, C., 1988. Effects of aridity on plant diversity in the northern Chilean Andes: results of a natural experiment. Ann. Mo. Bot. Gard. 75, 55–78.

Baker, P.A., Fritz, S.C., 2015. Nature and causes of Quaternary climate variation of tropical South America. Quat. Sci. Rev. 124, 31–47.

Baker PA, Fritz SC, Burns SJ, Ekdahl E, Rigsby CA (2009) The nature and origin of decadal to millennial scale climate variability in the southern tropics of South America: the Holocene record of Lago Umayo, Peru. In Vimeux F, Sylvestre F, Khodri M (eds), Past Climate Variability from the Last Glacial Maximum to the Holocene in South America and Surrounding Regions, Springer., pp. 301-322.

Bennet, K.D., 1996. Determination of the number of zones in a biostratigraphical sequence. New Phytol. 132, 155–170.

Berry, E.W., 1922. Late Tertiary plants from Jancocata, Bolivia. The John Hopkins University Studies in Geology 4, 205–221.

Blanco, S., Álvarez-Blanco, I., Cejuda-Figueiras, C., de Godos, I., Bécares, E., Muñoz, R., Guzman, H.O., Vargas, V.A., Soto, R., 2013. New diatom taxa from high-altitude Andean saline lakes. Diatom Research 28 (1), 13–27.

Brierly, C.M., Fedorov, A.V., 2016. Comparing the impacts of Miocene-Pliocene changes in inter-ocean gateways on climate: Central American Seaway, Bering Strait, and Indonesia. Earth Planet. Sci. Lett. 444, 116–130.

Brierly, C.M., Fedorov, A.V., Liu, Z., Herbert, T.D., Lawrence, K.T., LaRiviere, J.P., 2009. Greatly expanded tropical warm pool and weakened Hadley Circulation in the Early Pliocene. Science 323, 1714–1718.

Brown CA (2008) Palynological Techniques. Dallas, American Association of Stratigraphic Palynologists Foundation, 137 p.

Bullock, P., Fedoroff, N., Jongerius, A., Stoops, G., Babel, U., 1985. Handbook for Soil Thin-section Description. (Waine Research).

Bush, M.B., Weng, M.B., 2006. Introducing a new (freeware) tool for palynology. J. Biogeogr. 34, 377–380.

Charrier, R., Chávez, A.N., Elgueta, S., Hérail, G., Flynn, J.J., Croft, D.A., Wyss, A.R., Riquelme, R., García, M., 2005. Rapid tectonic and paleogeographic evolution of the Chucal anticline and the Chucal-Lauca Basin in the Altiplano of Arica, northern Chile. J. S. Am. Earth Sci. 19, 35–54.

Chong, Díaz G., Mendoza, M., García-Veigas, J., Pueyo, J.J., Turner, P., 1999. Evolution and geochemical signatures in a Neogene forearc evaporitic basin: the Salar Grande (Central Andes of Chile). Palaeogeogr. Palaeoclimatol. Palaeoecol. 155, 39–54.

Cocquyt, C., 2004. *Staurophora caljonii* spec. nov. (Bacillariophyceae, Anomoeoneidaceae), a new halophilic diatom species from sub-recent lake deposits in Kenya. Hydrobiologia 511 (1–3), 37–46.

Cohen A, McGlue MM, Ellis GS, Zani H, Swarzenski PW, Assine ML, Silva A (2015) Lake formation, characteristics, and deposystems: a synthesis of the modern Andean orogen and its associated basins, In DeCelles PG, Ducea MN, Carrapa B, Kapp PA (eds) Geodynamics of a Cordilleran Orogenic System: The Central Andes of Argentina and Northern Chile, Geological Society of America Memoir, 212.

de Wet, C.B., Godfrey, L., de Wet, A.P., 2015. Sedimentology and stable isotopes from a lacustrine-to-palustrine limestone deposited in an arid setting, climatic and tectonic factors: Miocene-Pliocene Opache Formation, Atacama Desert, Chile. Palaeogeogr. Palaeoclimatol. Palaeoecol. 426, 46–67.

de Wet CB, de Wet AP, Godfrey L, Driscoll E, Patzkowsky S, Xu C, Gigliotti S, Feitl M 2019

(in review) Pliocene short-term climate changes preserved in continental palustrine carbonates: Western Opache Formation, Atacama Desert, Chile. *GSA Bulletin*.
Doher, L.I., 1980. Palynomorph preparation procedures currently used in the paleontology and stratigraphy laboratories. U.S. Geological Survey. Geological Survey Circular 830, 1–28.
Ehlers, T.A., Poulsen, C.J., 2009. Influence of Andean uplift on climate and paleoaltimetry estimates. Earth Planet. Sci. Lett. 281, 238–248.
Fægri, K., Iversen, J., 1989. Textbook of Modern Pollen Analysis. Munksgaard, Copenhagen.
Fedorov, A.V., Dekens, P.S., McCarthy, M., Ravelo, A.C., deMenocal, P.B., Varreiro, M., Pacanowski, R.C., Philander, S.G., 2006. The Pliocene Paradox (mechanisms for a permanent El Niño). Science 312, 1485–1489.
Fedorov, A.V., Brierly, C.M., Lawrence, K.T., Liu, Z., Dekens, P.S., Ravelo, A.C., 2013. Patterns and mechanisms of early Pliocene warmth. Nature 496, 43–52.
Fiorella, R.P., Poulsen, C.J., Pillco Zolá, R.S., Barnes, J.B., Tabor, C.R., Ehlers, T.A., 2015. Spatiotemporal variability of modern precipitation $\delta^{18}O$ in the central Andes and implications for paleoclimate and paleoaltimetry estimates. Journal of Geophysical Research: Atmospheres 120, 4630–4656.
Fontes, J.C., Boulange, B., Carmouze, J.P., Florkowski, T., 1979. Preliminary oxygen-18 and deuterium study of the dynamics of Lake Titicaca. In: Mortimer, C. (Ed.), Application of Nuclear Techniques to the Study of Lake Dynamics. IAEA, Vienna, pp. 145–150.
Fritz, S.C., 2013. Salinity and climate reconstructions from continental lakes. In: Elias, S.A. (Ed.), Encyclopedia of Quaternary Science Volume 1. Elsevier, Amsterdam, pp. 507–515.
Fritz, S.C., Baker, P.A., Seltzer, G.O., Ballantyne, A., Tapia, P., Cheng, H., Edwards, R.L., 2007. Quaternary glaciation and hydrologic variation in the South American tropics as reconstructed from the Lake Titicaca drilling project. Quat. Res. 68, 410–420.
Fritz, S.C., Cumming, B.F., Gasse, F., Laird, K.R., 2010. Diatoms as indicators of hydrologic and climatic change in saline lakes. In: Smol, J.P., Stoermer, E.F. (Eds.), The Diatoms: Applications for the Environmental and Earth Sciences, 2nd edition. Cambridge University Press, Cambridge.
García, M., Riquelme, R., Farías, M., Hérail, G., Charrier, R., 2011. Late Miocene-Holocene canyon incisión in the western Altiplano, northern Chile: tectonic or climatic forcing? J. Geol. Soc. Lond. 168, 1047–1060.
Garreaud, R.D., 2009. The Andes climate and weather. Adv. Geosci. 7, 1–9.
Garreaud, R.D., Vuille, M., Compagnucci, R., Marengo, J., 2009. Present-day south American climate. Palaeogeogr. Palaeoclimatol. Palaeoecol. 281 (3–4), 180–195.
Garzione, C.N., Molnar, P., Libarkin, J.C., MacFadden, B.J., 2006. Rapid late Miocene rise of the Bolivian Altiplano: evidence for removal of mantle lithosphere. Earth Planet. Sci. Lett. 241, 543–556.
Garzione, C.N., Auerbach, D.J., Smith, J.J., Rosario, J.J., Passey, B.H., Jordan, T.E., Eiler, J.M., 2014. Clumped isotope evidence for diachronous surface cooling of the Altiplano and pulsed surface uplift of the Central Andes. Earth Planet. Sci. Lett. 393, 173–181.
Gasse, F., Fontes, J.C., Plaziat, J.C., Carbonel, C., Kaczmarska, I., De Deckker, P., Soulié-Marsche, I., Callot, Y., Dupeuble, P.A., 1987. Biological remains, geochemistry and stable isotopes for the reconstruction of environments and hydrological changes in the Holocene lakes from north Sahara. Palaeogeogr. Palaeoclimatol. Palaeoecol. 60, 1–46.
Gat, JR, 1995. Stable isotopes and the water balance of fresh and saltwater lakes. In: Lerman, A, Imboden DM, Gat JR (eds), Physics and Chemistry of Lakes, 2nd edition. Springer-Verlag, Berlin, 334 pp.
Gaupp, R., Kött, A., Wörner, G., 1999. Palaeoclimatic implications of Miocene-Pliocene sedimentation in the high-altitude intra-arc Lauca Basin of northern Chile. Palaeogeogr. Palaeoclimatol. Palaeoecol. 151, 79–100.
Gehrels, G., 2014. Detrital zircon U-Pb geochronology applied to tectonics. Annu. Rev. Earth Planet. Sci. 42, 127–149.
Ghosh, P., Garzione, C.N., Eiler, J.M., 2006. Rapid uplift of the Altiplano revealed through ^{13}C-^{18}O bonds in paleosol carbonates. Science 311 (5760), 511–515.
Giralt, S., Moreno, A., Bao, R., Sáez, A., Prego, R., Valero-Garcés, B.L., Pueyo, J.J., González-Sampériz, P., Taberner, C., 2008. A statistical approach to disentangle environmental forcings in a lacustrine record: the Lago Chungará case (Chilean Altiplano). J. Paleolimnol. 40, 195–215.
Gonfiantini, R., Cioni, R., Paredes, M., Campos, J., Collas, M., Gaita, A., Rojas, R., Quintanilla, J., et al., 2002. Hydrochemical and isotope study of Lake Titicaca. Study of Environmental Change Using Isotope Techniques. IAEA, Vienna, pp. 231–241.
Gosling, W.D., Mayle, F.E., Tate, N.J., Killeen, T.J., 2009. Differentiation between Neotropical rainforest, dry forest, and savannah ecosystems by their modern pollen spectra and implications for the fossil pollen record. Review of Paleobotany and Palynology 153, 70–85.
Gregory-Wodzicki, K.M., 2000. Uplift history of the Central and Northern Andes: a review. GSA Bull. 112 (7), 1091–1105.
Gregory-Wodzicki, K., McIntosh, W.C., Valasquez, K., 1998. Climatic and tectonic implications of the late Miocene Jakokkota flora, Bolivian Altiplano. Journal of South American Sciences 11, 533–560.
Hammer UT (1986) Saline Lake Ecosystems of the World. Dordrecht, The Netherlands: Dr. W. Junk Publishers: 616p.
Hammer, U.T., Shamess, J., Haynes, R.C., 1983. The distribution and abundance of algae in saline lakes of Saskatchewan, Canada. Hydrobiologia 105, 1–26.
Hammer, U.T., Sheard, J.S., Kranabetter, J., 1990. Distribution and abundance of littoral benthic fauna in Canadian prairie saline lakes. Hydrobiologia 197, 173–192.
Heusser, C.J., 1971. Pollen and Spores of Chile, Modern Types of Pteridophyta, Gymnospermae, and Angiospermae. The University of Arizona Press, Tucson.
Houk, V., 2003. Atlas of freshwater centric diatoms with a brief key and descriptions. Part I. Melosiraceae, Orthoseiraceae, Paraliaceae, and Aulacoseiraceae. Czech Phycology, Supplement 1, 1–11.
Kirk-Lawlor, N.E., Jordan, T.E., Rech, J.A., Lehmann, S.B., 2013. Late Miocene to Early Pliocene paleohydrology and landscape evolution of Northern Chile 19° to 20°S. Palaeogeogr. Palaeoclimatol. Palaeoecol. 387, 76–90.
Kött, A., Gaupp, R., Wörner, G., 1995. Miocene to recent history of the western Altiplano in the northern Chile revealed by lacustrine sediments of the Lauca Basin (18°15′-18°40′S/69°30′-69°-05′W). Geologische Rundshau 84, 770–780.
Krammer K, Lange-Bertalot H (1986) Bacillariophyceae. 1. Teil: Naviculaceae. In Ettl H, Gerloff J, Heynig H, Mollenhauer D (eds) Süwasser flora von Mitteleuropa, Band 2/1. Gustav Fischer Verlag. Stuttgart, New York. 876 p.
Krammer K, Lange-Bertalot H (1988) Bacillariophyceae. 2. Teil: Bacukkaruaceae, Epithemiaceae, Surirellaceae. In Ettl H, Gerloff J, Heynig H, Mollenhauer D (eds) Süwasser Flora von Mitteleuropa, Band 2/2. VEB Gustav Fischer Verlag. Jena. 596 p.
Krammer K, Lange-Bertalot H (1991a) Bacillariophyceae. 3. Teil: Centrales, Fragilariaceae, Eunotiaceae. In Ettl H, Gerloff J, Heynig H, Mollenhauer D (eds) Süwasser flora von Mitteleuropa, Band 2/3. Gustav Fischer Verlag. Stuttgart, Jena. 576 p.
Krammer K, Lange-Bertalot H (1991b) Bacillariophyceae. 4. Teil: Achnanthaceae, Kritische Ergänzungen zu Navicula (Lineolatae) und Gomphonema, Gesamtliteraturverzeichnis Teil 1-4. In Ettl H, Gärtner G, Gerloff J, Heynig H, Mollenhauer D (eds) Süwasser flora von Mitteleuropa, Band 2/4. Gustav Fischer Verlag. Stuttgart, Jena. 437 p.
Kuentz, A., Galan de Mera, A., Ledru, M.P., Thouret, J.C., 2007. Phytogeographical data and modern pollen rain of the puna belt in southern Peru (Nevado Coropuna, Western Cordillera). J. Biogeogr. 34 (10), 1762–1776.
Labraga, J., 1997. The climate change in South America due to doubling in the CO_2 concentration: intercomparison of general circulation model equilibrium experiments. Int. J. Climatol. 17, 377–398.
Lambrinos, J.G., Kleier, C., Rundel, P.W., 2006. Plant community variation across a puna landscape in the Chilean Andes. Rev. Chil. Hist. Nat. 79 (2), 233–243.
Lenters, J., Cook, K., 1995. Simulation and diagnosis of the regional summertime precipitation climatology of South America. J. Clim. 8, 2988–3005.
Liu X, Battisti D, White RH, Baker PA 2019 (in review). South American climate during the early Eocene: impact of a narrower Atlantic and higher atmospheric CO2. Journal of Climate.
Maidana, N.I., Seeligmann, C., Morales, M.R., 2011. El género *Navicula sensu stricto* (Bacillariophyceae) en humedales de altura de Jujuy, Argentina. The Bulletin of the Botanical Society of Argentina 46 (1–2), 13–29.
Markgraf, V., D'Antoni, L., 1978. Pollen Flora of Argentina, Modern Spore and Pollen Types of Pteridophyta. The University of Arizona Press, Gymnospermae and Angiospermae.
May, G., Hartley, A.J., Stuart, F.M., Chong, G., 1999. Tectonic signatures in arid continental basins: an example from the Upper Miocene-Pleistocene Calama Basin, Andean forearc, northern Chile. Palaeogeogr. Palaeoclimatol. Palaeoecol. 151, 55–77.
Mulch, A., Uba, C.E., Strecker, M.R., Schoenberg, R., Chamberlain, P., 2010. Late Miocene climate variability and surface elevation in the central Andes. Earth Planet. Sci. Lett. 290, 173–182.
Munsell Color Firm (2010) Munsell Soil Color Charts: with Genuine Munsell Color Chips.
O'Neil, J.R., Clayton, R.N., Mayeda, T.K., 1969. Oxygen isotope fractionation between divalent metal carbonates. J. Chem. Phys. 51, 5547–5558.
Ortuño, T., Ledru, M.P., Cheddadi, R., Kuentz, A., Favier, C., Beck, S., 2011. Modern pollen rain, vegetation and climate in Bolivian ecoregions. Rev. Palaeobot. Palynol. 165, 61–74.
Palazzesi, L., Gottschling, M., Barreda, V., Weigand, M., 2012. First Miocene fossils of Vivianiaceae shed new light on phylogeny, divergence times, and historical biogeography of Geraniales. Biol. J. Linn. Soc. 107, 67–85.
Poulsen, C.J., Jeffrey, M.L., 2011. Climate change imprinting on stable isotopic compositions of high-elevation meteoric water cloaks past surface elevations of major orogens. Geology 39, 595–598.
Poulsen, C.J., Ehlers, T.A., Insel, N., 2010. Onset of convective rainfall during gradual late Miocene rise of the Central Andes. Science 328 (5977), 490–493.
Quade, J., Carter, M.L., Ojha, T.P., Adam, J., Harrison, T.M., 1995. Late Miocene environmental change in Nepal and the northern Indian subcontinent: stable isotopic evidence from paleosols. Bulletin for the Geological Society of America 107 (12), 1381–1397.
Rada, O., Romero, S., Tejada Miranda, F., 1997. Analysis of climate scenarios for Bolivia. Clim. Res. 9, 115–120.
Reese, C.A., Liu, K.B., 2005. A modern pollen rain study from the central Andes region of South America. J. Biogeogr. 32, 709–718.
Roubik, D.W., Moreno, P., 1991. Pollen and Spores of Barro Colorado Island. Missouri Botanical Garden Press.
Rozanski, K., Araguás, L., 1995. Spatial and temporal variability of stable isotope composition of precipitation over the south American continent. Bulletin de l'Institut Français d'Études Andines 24, 379–390.
Rumrich, U., Lange-Bertalot, H., Rumrich, M., 2000. Diatoms of the Andes: From Venezuela to Patagonia/tierra Del Fuego: And Two Additional Contributions. Königstein, Germany.
Rundel, P.W., Palma, B., 2000. Preserving the unique puna ecosystem of the Andean Altiplano: Lauca National Park, Chile. Mt. Res. Dev. 20, 262–271.
Sáez, A., Cabrera, L., Jensen, A., Chong, G., 1999. Late Neogene lacustrine record and palaeogeography in the Quillagua-Llamara basin, Central Andean fore-arc (northern Chile). Palaeogeogr. Palaeoclimatol. Palaeoecol. 151, 5–37.
Sáez, A., Cabrera, L., Garcés, M., van den Bogaard, P., Jensen, A., Gimeno, D., 2012. The stratigraphic record of changing hyperaridity in the Atacama Desert over the last 10 Ma. Earth Planet. Sci. Lett. 355–356, 32–38.

Smith AJ, Horne DJ (2016) Ostracoda of the Nearctic. In: Thorp J, Rogers DC (eds.), Ecology and General Biology: Thorp and Covich's Freshwater Invertebrates, Volume 2, Chapter 16, Academic Press, pp. 477-513.

Sylvestre, F., Servant-Vildary, S., Roux, M., 2001. Diatom-based ionic concentration and salinity models from the south Bolivian Altiplano (15-32°S). J. Paleolimnol. 25, 279–295.

Taylor, J.C., Harding, W.R., Archibald, C.G.M., 2007. An Illustrated Guide to Some Common Diatom Species From South Africa. WRC, Pretoria, South Africa.

Thompson, L.G., Davis, M.E., Mosley-Thompson, E., Sowers, T.A., Henderson, K.A., Zagorodnov, V.S., Lin, P.N., Mikhalenko, V.N., Campen, R.K., Bolzan, J.F., Cole-Dai, J., Francou, B., 1998. A 25,000 year tropical climate history from Bolivian ice cores. Science 282, 1858–1864.

Traverse A (2007) Paleopalynology. Springer, Dordrecht, 813 p.

Vélez, M.L., Jaramillo, C., Salazar-Ríos, A., Benito, X., Fritz, S., Tapia, P., Lubiniecki, D., Kar, N., Escobar, J., 2017. Aquatic ecosystems in a newly formed ecospace: Early Pliocene lakes in the Central Andean Altiplano. Palaeogeogr. Palaeoclimatol. Palaeoecol. 490, 218–226.

Wang, Q., Yang, X., Hamilton, P.B., Zhang, E., 2012. Linking spatial distributions of sediment diatom assemblages with hydrological depth profiles in a plateau deep-water lake system of subtropical China. Fottea 12, 59–73.

Wara, M.W., Ravela, A.C., Delaney, M.L., 2005. Permanent El Niño-like conditions during the Pliocene warm period. Science 309 (5735), 758–761.

Wörner, G., Harmon, R.S., Davidson, J., Moorbath, S., Turner, D.L., McMillan, N., Nye, C., Lopez-Escobar, L., Moreno, H., 1988. The Nevados de Payachata volcanic region (18°S/69°W, N. Chile): I. Geological, geochemical and isotopic observations. Bull. Volcanol. 30, 287–303.

Wörner, G., Hammerschmidt, K., Henjes-Kunst, F., Lexaun, J., Wilke, H., 2000. Geochronology ($^{40}Ar/^{39}Ar$, K-Ar and He-exposure ages) of Cenozoic magmatic rocks from Northern Chile (18-22°S): Implications for magmatism and tectonic evolution of the central Andes. Revista Geológica de Chile 27 (2), 205–240.

Zachos, J., Pagani, M., Sloan, L., Thomas, E., Billups, K., 2001. Trends, rhythms, and aberrations in global climate 65 Ma to present. Science 292, 686–693.

Zhang, Y.G., Pagani, M., Liu, Z., Bohaty, S.M., DeConto, R., 2013. A 40-million-year History of Atmospheric CO_2. Mathematical, Physical, and Engineering Sciences, Philosophical Transactions, pp. 3711–3720.

Zhisheng, A., Kutzbach, J.E., Prell, W.L., Porters, S.C., 2001. Evolution of the Asian monsoons and phased uplift of the Himalaya-Tibetan plateau since the Late Miocene times. Nature 411, 62–66.